Memoirs of the Faculty of Engineering, Okayama University, Vol.25, No. 1, pp.37-50, November 1990

Second Harmonic Detection of Atmospheric Trace Gases with a Train-Pulse Driven Lead-Salt Tunable Diode Laser for an Operation at Peltier Cooling Temperature

Moncef BOUZIDI[*,†], Ryuji KOGA[**], Osami WADA[**],
Naoki KAGAWA[*], Xu Hai[††], Megumi KOSAKA[**] and Hiroya SANO[†††]

(Received November 1 , 1990)

SYNOPSIS

Is proposed a tunable diode laser absorption spectrometer system which employs a pulsed current to drive the diode laser still implementing a second-harmonic detection methods enhancing a signal to noise up to 104 times that the case without it. This system affords the lead-salt diode laser a higher operating temperature which allows a more compact deep cooling system. A principle is based on employing a gated integrator between the preamplifier and the lock-in amplifier. Investigations are made on the optimum selection of the gating aperture time interval as determined by response time of the infrared detector and the pulse width of the laser driving current.

1. INTRODUCTION

Lead-salt diode lasers have found widespread application in infrared spectrometry, due to their large emission range and quick tunability that can

*The Graduate School of Natural Science and Technology, **Department of Electrical and Electronic Engineering, †Permanent address: ENSET, University of Tunis, Tunisia, ††Measurement and Test Center, North-East Normal University, Changchun, China, †††Faculty of Engineering, Fukuyama University.

be obtained simply by varying either the operating temperature or the drive current[1]. These important features have been exploited particularly in detection of low pollutant concentrations. In this case, the second derivative method is generally used to suppress unwanted signals, implemented by modulating the laser frequency and employing a lock-in amplifier[2].

In previous papers [3,4], we reported about a cw mode operating derivative spectrometer capable of real time, *in-situ*, and non-contact measurements of trace gases in the atmosphere. Its performance was evaluated with regard to the detection of methane (CH_4) when using a PbSnTe TDL emitting at the 7μm band, and a precision as good as 80 ppb·m was obtained. However the monitoring system was limited to indoor measurements due to the use of a bulky refrigerator, inevitable for the cooling of the diode laser.

Second harmonic detection method with a pulsed mode laser system combine both the portability and the sensitivity. Contrary to cw operation where lasers require usually deep cooling, operation in pulsed mode makes it possible for lasers to work under higher temperatures in which case rather compact devices are usable for the cooling. This is favorable for a hand-held monitoring system.

Recent advances in the technology of lead-salt lasers have improved their emission characteristics. Lasers are now available which provide higher output power with reduced threshold current in single mode operation[5]. Furthermore, the operation temperature can be increased nearly up to room temperature especially under pulsed conditions [6]. Operation of a pulsed DH PbSSe laser with Peltier coolers has been already achieved[7] for use for a portable atmospheric gas monitoring.

This paper deals with a portable system using a pulsed laser for monitoring atmospheric trace gases and examine the highest sensitivity available. A temporal integration technique for S/N enhancement is discussed and factors which currently govern the sensitivity of the system are investigated. It is shown that with possible infrared detectors a measurement accuracy of about 1ppb·m is expected to be attainable.

2. NOISE AND ITS SUPPRESSION IN A PULSE-OPERATED SYSTEM

Both optical and electrical noises determine the error in the obtained gas density with a laser spectrometry system. In a former work [8],

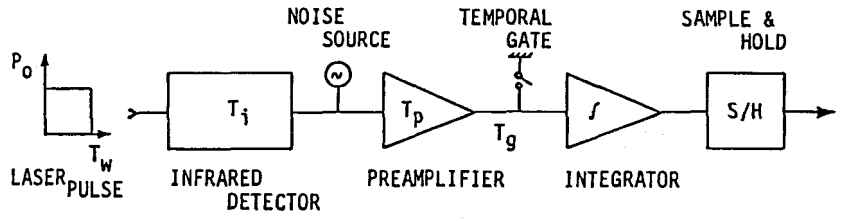

Fig.1 Preconditioner model for random noise analysis.

authors have reported their success in reducing the effects of etalon fringes which dominate the optical noise to a value of as low as 10^{-6} in terms of absolute absorption. Hereafter, the electrical noise is examined using the model illustrated in Fig.1, where only an infrared detector and a preamplifier, are taken into account as predominant noise sources. However though noise from the latter can be reduced to the minimum by adequate electronic design, it is not the case for infrared detectors for which noise reduction rely on their fabrication. It becomes necessary therefore, to use techniques for suppression of such noise.

In case when the timing when the signal should arrives is known, a matched filter gives rise to the maximum signal to noise ratio (SNR) in the electrical signal processing. A complex convolver is however, necessary to be employed, which prevents this method to be immediately utilized. The temporal gate integration is a suboptimal alternative to the matched filter and is the more effective as the signal profile is approaching a rectangle shape that is generated by the switching action.

In the following, an expression for the signal to noise ratio relative to the absolute absorption will be derived, parameters are examined for its optimization, and experimental results confirming suppression of noise with the integration method will be presented.

Since a photoconductive detector is employed, generation-recombination noise and Johnson noise are the fundamental noise mechanisms [10], hence for the frequency region of interest between 1kHz and 1.5MHz the noise signal, whose bandwidth distributes over enough wider beyond that of the signal, can be considered stationary with white and Gaussian characteristics as depicted in Fig.2.

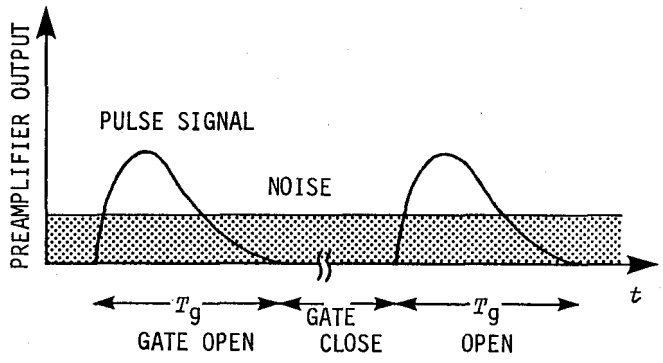

Fig.2 Principle of noise suppression by simple integration.

With the temporal gate integrator used as in Fig.1, by switching the gate ON and OFF synchronized to the laser driving current, integration is achieved only over the smallest interval Tg that encloses the pulse signal corresponding to the optical input to the infrared detector, as a result noise between two successive pulses is discarded. Noise in the same interval Tg as the signal, which is off the reach of the above technique, is suppressed with the well known second harmonic detection, and also with the adjoint spectra invented by the authors as a tool against spectral interference [11].

Let us formulate the noise to signal ratio at the integrator output with the model of Fig.1, where the infrared detector and a preamplifier have a transfer functions of first order with time constants T_i and T_p, respectively. Assuming that noise from the detector is not band-limited, an equivalent noise source of power spectral density N^2 is represented by the voltage signal of Fig.1. When expressed in terms of the incident light power, N^2 is given by,

$$N^2 = A_d/D^{*2} + e_n^2/R_e^2, \tag{1}$$

where, A_d, D^* and R_e are the area, detectivity and responsivity of the detector, respectively, while e_n is the noise equivalent voltage of the preamplifier. By using the spectral density function at the output of the preamplifier and the related autocorrelation function for the case of a stationary random process [12], the variance of the noise integrated over the time interval T_g is derived as,

$$\mathrm{var}(n) = (N^2)\ [\ T_g - T_p\{\ 1 - \exp(-T_g/T_p)\}]. \tag{2}$$

On the other hand, the laser signal which falls on the detector is processed by the system depicted in Fig.1, and the sample-holder output that is a time integral of the preamplifier output over the interval T_g becomes,

$$P = \int s(t)\mathrm{d}t = P_o\ [\ T_w + (1/T_p - T_i)\{T_p^{\,2} \exp(-T_g/T_p)(1-\exp T_w/T_p)$$

$$- T_i^{\,2} \exp(-T_g/T_i)(1-\exp T_w/T_i)\}], \tag{3}$$

which is obtained under the legitimate condition $T_g > T_w$, where T_w is the laser pulse width. The SNR relative to the preconditioner is then deduced as,

$$\mathrm{SNR} = P^2 \ / \ \mathrm{var}(n). \tag{4}$$

Figure 3 gives the SNR as a function of the integral duration T_g with the laser pulse width T_w and the detector response time T_i as parameters respectively in (a) and (b). Values of other parameters related to the actual experimental system and involved in the computation are indicated in Table 1. Inspection of these sets of curves shows that in general, higher values of the SNR require wider width T_w of the laser pulse and smaller response time T_i of the detector. Also for the special case of the presented system where the response time T_i of the detector is larger than both the laser pulse width T_w and the response time T_p of the preamplifier, the optimal value of the gating

Table 1. Parameters used in SNR computation

A_d	infrared detector active area	400×400μm
D^*	infrared detector detectivity	3.8×10^9 cm$\sqrt{\mathrm{Hz}}$/W
R_e	infrared detector responsivity	3.0×10^2 V/W
T_i	infrared detector time constant	30nsec ~ 10μsec
e_n	preamp.equiv.noise voltage	10mV/$\sqrt{\mathrm{Hz}}$
P_o	received power at infrared det.	1mW
T_p	Preamplifier response time	50nsec
T_w	Laser pulse width	300nsec
T_g	Gating time	10^2 ~ 10^6nsec

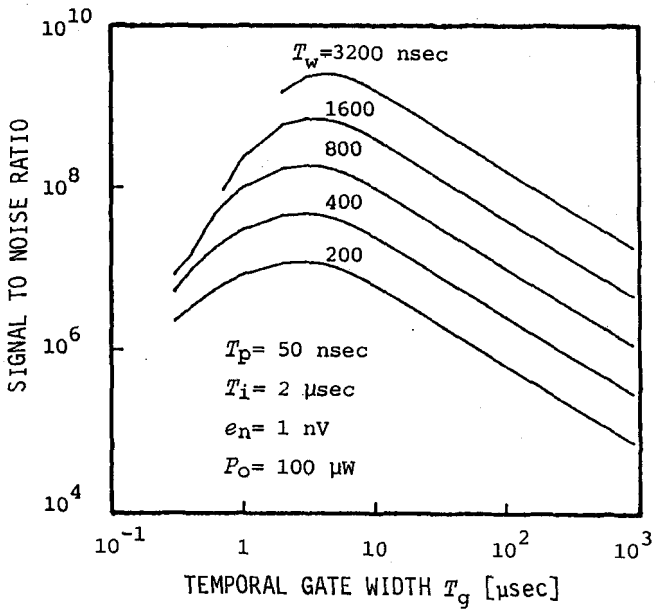

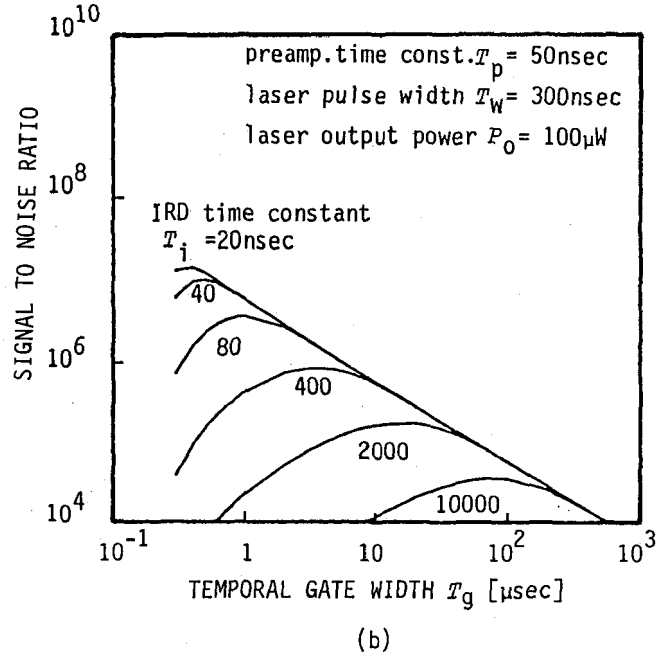

Fig.3 (a) Signal to noise ratios as functions of temporal gate width T_g with parameters of laser pulse widths, and (b) with parameters of IRD time constant T_i.

time T_g which yields a maximum SNR occurs nearly at $T_g=T_i$, Fig.3(a).

Beside the time parameters discussed above, there exist other parameters which also control the performance of the system as shown by eq.(4). It is clear that less noise arising at both the detector and the preamplifier, and higher incident laser power will further enhance the SNR. Hereafter the ultimate capability of the system is examined in terms of the SNR, as far as the state of the art of the involved devices is concerned.

As preamplifiers having noise equivalent voltage lower than 1nV/ Hz with bandwidths expanding above 100MHz became possible[13], the corresponding contribution in the system noise can be considered as the minimum limit attainable. Therefore, further enhancement in the SNR will rely essentially on the improvement of the IRD devices. After remarkable advances in their technology, infrared detectors are now available with a detectivity higher than 10^{11}cm Hz/W, an area as small as 0.05 mm^2 and a response time in the nanosecond order[13].

Figure 4 provides a comparison of the SNR of the system with the IRD we employed for our experiments and other possible IRD devices, which characteristics are listed in table 2. This shows an enhancement of the SNR which may reach as high as 4 orders of magnitude by selecting a detector with proper parameters.

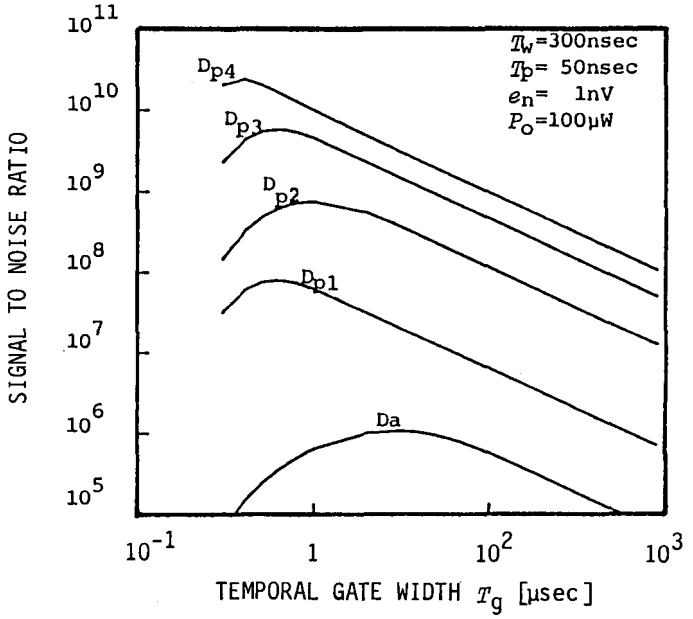

Fig.4 Signal to noise ratios attainable with actual IRD's.

Table 2. Characteristics of selected IRD devices used in computation of SNR in Fig.4.

IRD	A_d [mm^2]	D* [cm$\sqrt{Hz}$/W]	T_i [nsec]
D_a	0.16	3.8×10^{10}	2000
D_{p1}	0.10	3.0×10^{10}	200
D_{p2}	0.05	3.0×10^{10}	500
D_{p3}	0.05	6.0×10^{10}	200
D_{p4}	0.05	8.7×10^{10}	25

IRD: infrared detector; D_a: available device; D_p: possible device.

3. EXPERIMENTAL APPARATUS

The experimental set-up is illustrated schematically in Fig.5, which is almost the same with that used for the cw-mode operated system reported before[3,4], with few modifications carried at the laser current driver and also by addition of a gated integrator for noise suppression in the pulsed mode operation.

The TDL is a buried DH $Pb_{1-x}Sn_xTe$ mounted in a cryogenic refrigerator which can be temperature controlled in the range of 100 to 15K at a stability rate of 1.5mK/min. It emits at the 7.6μm band and can be easily tuned from 6.6 to 8.6μm where methane has a strong absorption band, $\nu 4$ band.

Figure 6 shows the waveform of the laser drive current. It is the sum of three components: a laser driving pulse current i_p, a heat-up current i_h, and a modulation current i_m. Without i_p applied, the emission wavelength through the junction temperature is determined by the sum of i_h and i_m. The heat-up current i_h is controlled in a staircase manner so that it allows a coarse adjustment of the laser wavelength over the spectral region of interest. The three-state square waveform shown in the lower part of Fig.6 represents the profile of the modulation current i_m.

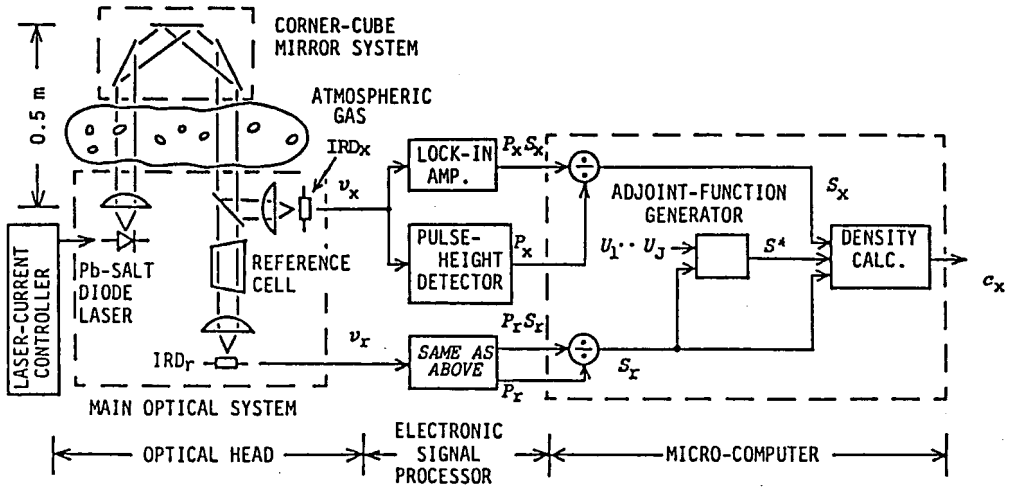

Fig.5 A tunable diode laser spectrometry system to measure density of atmospheric methane with double optical paths.

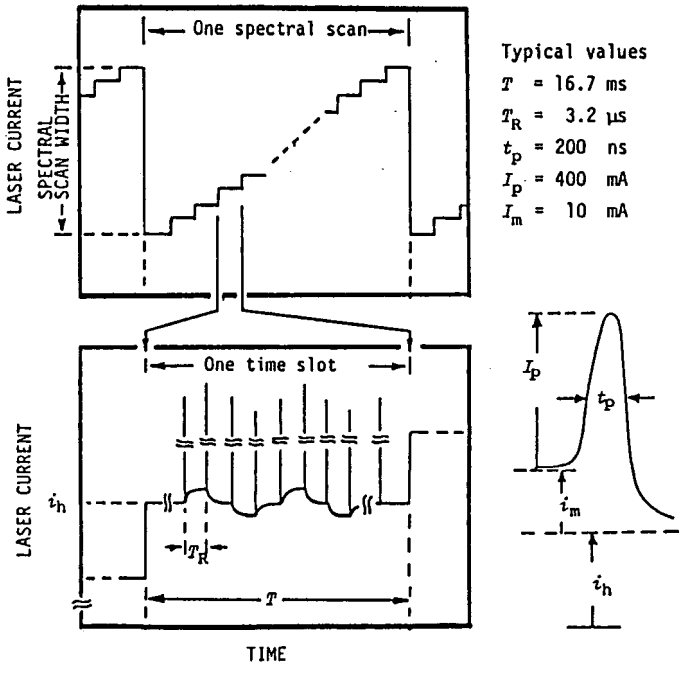

Fig.6 Temporal program of driving current applied to the diode laser. The current is a superposition of a heat-up current i_h, a modulation current i_m, and the pulse current i_p for lasing.

4. EXPERIMENTAL RESULTS

4.1 Noise suppression by integration technique in pulse mode operation

In order to confirm theoretical results on suppression of noise by an integration technique in the pulse-mode operation, as discussed above, an experimentation to measure an absorption spectrum of methane has been made. Figure 7 shows the $2f$ spectrum for three values of the gate duration T_g when a 3 Torr 100% 10cm methane gas cell was employed.

As a result it may be verified easily that noise has been considerably suppressed where T_g is equal to T_i, which corresponds to the optimal value of the gate duration that has been found to maximize the SNR in our system.

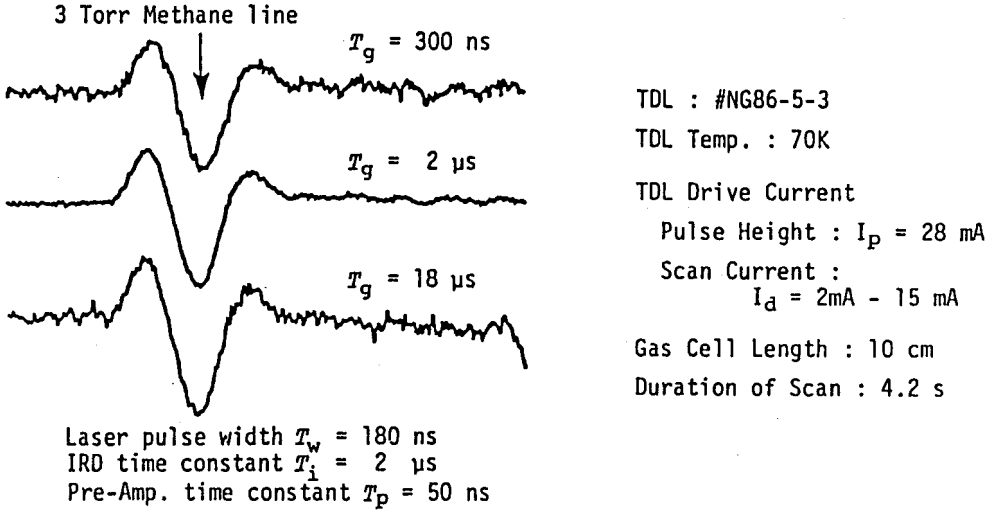

Fig.7 Measured second harmonic spectra of 3 Torr, Doppler-limited line spectra with different temporal gate aperture. The best SNR is attained to T_g=2μs, which corresponds to the time constant of the IRD employed.

4.2 Measurement of methane gas density

Figure 8 shows an example of spectrum of standard methane of 9410ppm at 1atm in a 3cm long cell, which has been used for gas density measurements, and the corresponding results. Note that the spectrum is sub-

ject to significant random noise. The inquired gas density was computed with an equation

$$c_x = (c_r \cdot L_r / L_x) \cdot \langle S^*, S_x \rangle / \langle S^*, S_r \rangle, \tag{5}$$

where suffixes x and r stand for the measurement leg and the reference leg respectively, c denotes the gas density and L the optical path length. Spectra S_x and S_r are second harmonic spectra recorded for the same laser frequency scanning, and normalized by each power. The weight distribution S^*, referred to as "adjoint spectrum" by the authors, is a powerful tool against spectral interferences that deteriorate measurement accuracy.

Repeated experiments with the conditions of Fig. 8, resulted in an accuracy of 8ppm·m for the experimental system in its primary stage.

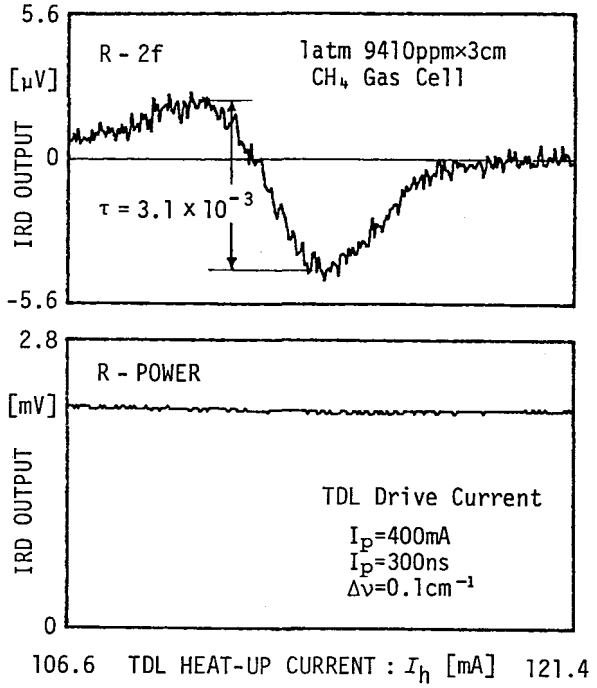

Fig.8 A second-harmonic spectrum(upper) and a power spectrum(lower) of a pressure broadened methane. The asymmetry found in the spectrum is due to the thermal constant of the diode laser, which drives the laser frequency from left to right during a pulse shot.

4.3 Discussion and Conclusion

This paper presents a possible portable system for monitoring atmospheric trace gases based on a pulsed laser, and examined its highest sensitivity when using a temporal gate integration for suppression of noise.

Analytical investigations suggest that by optimizing the integration duration T_g and selecting proper IRD devices, it is possible to enhance the signal to noise ratio by more than 4 orders of magnitude. This yields an error on the measured value of the absolute absorption as small as 1.4×10^{-7} making the system accuracy etalon fringe limited. It also suggests that gas density measurement with a pulsed-mode system is achievable with a 1.4 ppb·m (rms) level accuracy if an absorption coefficient of the involved methane line is supposed to be $10^2 m^{-1}$ at an atmospheric pressure.

REFERENCES

[1]. H.Prier, Appl.Phys., Vol.20, 189-206(1979).
[2]. J.Reid and D.Labrie, Appl.Phys., Vol.B26, 203-210(1981).
[3]. H.Sano, R.Koga and M.Kosaka, J.J.Appl.Phys., Vol.22, 1883-1888(1983).
[4]. R.Koga, M.Kosaka, H.Sano, Optics and Laser Technology, 139-144(1985).
[5]. A.DUTTA, long wavelength semiconductor lasers , Van Nostrand Reinhold(1986).
[6]. B.Spranger et al., Appl.Phys.Lett., Vol.53, 2582-2583(1988).
[7]. K.Shinohara, Monitoring of Gaseous Pollutants by Tunable Diode Lasers, 77-84(1989).
[8]. R.Koga, S.Nagase, M.Kosaka, H.Sano, Memoirs of the school of Eng., Okayama Univ., Vol.15-2, (1981).
[9]. N.Mohanty, Random Signals Estimation and Identification Van Nostrand Reinhold books(1986).
[10].R.J.Keyes, Topics on Appl. Phys. , Opt.and Infrared Detectors, Springer-Verlag, Vol.19, (1977).
[11].H.Sano, R.Koga, Y.Tanada, M.Kosaka, Memoirs of the school of Eng., Okayama Univ., Vol.13, 195-207(1979).
[12].B.Piersol, Random Data 2nd Edition, Wiley Interscience (1986).
[13].Tokyo Instruments Co., Spectroscopic Analysis(1988) .

APPENDIX

In the preconditioner model of Fig.1, the infrared detector and the preamplifier are assumed to be the principal sources of noise. In the following is derived the expression of the signal to noise ratio(SNR) at the output of this circuit and deduce the SNR relative to absolute absorption.

To characterize the random noise generated, an equivalent noise source of voltage v_n and spectral density $S(f)=N^2$ is supposed to exist at the input of the preamplifier as in Fig.1. Variance of the noise after integration over Tg can be expressed as,

$$\mathrm{var}(n)= \mathrm{var}\left[\int_0^{T_g} x(t)\mathrm{d}t\right] = 2T_g\int_0^{T_g}(1-t/T_g)(R_x(t)-m_x)\mathrm{d}t, \tag{1-1}$$

where $R_x(t)$ is the autocorrelation of $x(t)$ expressed as,

$$\begin{aligned} R_x(t) &= 1/2\pi \int_{-\infty}^{\infty} [N^2/(1+w^2 T_p{}^2)]\exp(j\omega t)\mathrm{d}\omega, \\ &= N^2 \exp(-t/T_p)/2T_p \end{aligned} \tag{1-2}$$

and m_x is the mean value of the white noise $x(t)$.
By integrating and substituting for $R_x(t)$, we obtain

$$\mathrm{var}(n)= N^2 [T_g + T_p(\exp(-T_g/T_p) - 1)]. \tag{1-3}$$

In terms of the input light power to the IRD, the power spectral density of noise is given by

$$N^2 = A_d/D^{*2} + e_n{}^2/R_e{}^2, \tag{1-4}$$

where A_d, D^* and R_e are the area, detectivity and responsivity of the IRD respectively, while e_n is the noise equivalent voltage of the preamplifier. A complete expression of $\mathrm{var}(n)$ is then obtained as,

$$\mathrm{var}(n)= (A_d/D^{*2} + e_n{}^2/R_e{}^2) [T_g + T_p(\exp(-T_g/T_p) -1)]. \tag{1-5}$$

By using the same model of Fig.1 as above, a similar result is obtained for the response of the preconditioner to the input pulse signal of laser,

$$P = \int_0^{T_g} s(t)dt = P_0 [T_w + 1/(T_p - T_i) \{T_p^2 \exp(-T_g/T_p) (1-\exp T_w/T_p) - T_i^2 \exp(-T_g/T_i) (1-\exp Tw/T_i)\}]. \quad (1-6)$$

The SNR at the output of the integrator becomes therefore,

$$SNR = P^2/ \text{var}(n). \quad (1-7)$$

After being sampled and holded the output of the integrator is feeded to the lock-in amplifier (L.I.A.) where the second harmonic of the signal is to be extracted. When the filter bandwidth B is large compared to the integration time T of the phase shift detector(PSD), the resultant output of the L.I.A. converted to its input is,

$$\overline{d^2 \overline{P + V_n}} = (1/T) \int_0^T (d^2 P + V_n) dt, \quad (1-8)$$

where d^2 denotes the second harmonic generator.

Taking the variance yields,

$$\text{var}(\overline{d^2 \overline{P + V_n}}) = \text{var}(\overline{V_n}), \quad (1-9)$$

since the $d^2 P$ is steady signal.

Assuming that the sample-hold time T_{sh} is enough larger than the pulse signal width, the fluctuations in each interval T_{sh} may be considered as mutually independent, hence

$$\text{var}(\overline{V_n}) = \text{var}(\sum^M V_n/M) = (1/M)\text{var}(V_n), \quad (1-10)$$

where $M = T/T_{sh}$, the number of pulses over one time slot.
The resultant fluctuation $\delta\chi$ on the absolute absorption χ is then deduced as,

$$\text{var}(\delta\chi) = (1/M) \text{var}(V_n)/ P^2. \quad (1-11)$$